Quartz-Blazed Grating Applied on Autostereoscopic Display

Chien-Yue Chen, Qing-Long Deng, Bor-Shyh Lin, and Wen-Cheng Hung

***Abstract*—By applying reactive ion etching (RIE) to a blazed grating on quartz substrates, the grating can be utilized as a splitter in autostereoscopic displays. Furthermore, a solution for the pattern alignment on transparent substrates is also proposed. By measuring the diffraction efficiency and crosstalk between the left and right fields of view (FOV), the capability of the element to deliver stereoscopic images is demonstrated.**

***Index Terms*—Autostereoscopy, blazed grating, quartz.**

I. Introduction

RECENTLY, stereoscopic glasses have been superseded in the stereoscopic display industry by autostereoscopic display technology, which is more convenient and easily combined with current display systems. This technology has become the mainstream display product. Nevertheless, the most popular forms of the technology, the barrier and lenticular systems, have revealed technological defects. Barrier autostereoscopic devices present a fully stereoscopic sensation; however, the 22.40% brightness is unacceptable, and the increased brightness provided by the backlight consumes more energy [1]. Lenticular autostereoscopic displays, however, depend on attaching a lenticular lens to the panel to deliver horizontal images [2]. Differing from highly transparent and novel structures and to alleviate the disadvantages of barrier devices, the research team first proposed the concept of the diffractive optical element (DOE) in 2010 to apply a blazed grating to the splitter of autostereoscopic displays and thereby overcome the problem of diffractive elements being easily affected by optical wavelengths [3].

Blazed gratings are phase diffractive elements because they consist of periodical structures. Proper adjustment of the blazed angle allows the primary maximum of single slit diffractive factors and overlap of diffractive grating in a diffractive order of the intermediates in slits such that the diffractive grating in a specific diffractive order presents the largest diffraction efficiency [4], [5].

The common DOE process uses a micromachining technology, such as the LIGA (Lithographie, Galvanoformung, Abformung) process, which achieves several optical effects based on diffraction. Due to its light weight, small size, easy duplication, and low cost, it can achieve a specific function that traditional optical elements cannot [6]. Nevertheless, the multiple process steps used in the LIGA process cause cumulative errors and further damage the structure of the diffractive elements. As DOEs are sensitive to optical wavelengths, the error structure can apparently affect diffraction efficiency. In this case, both photolithography and reactive ion etching were utilized to produce a blazed grating on quartz substrates to implement the diffractive stereoscopic display and combine the 3D image source with a laser background for testing. However, it was difficult to produce the secondary optic shape of transparent substrates. Thus, this study proposed a solution for the multi-stage alignment of transparent substrates to successfully produce the DOE for autostereoscopic displays.

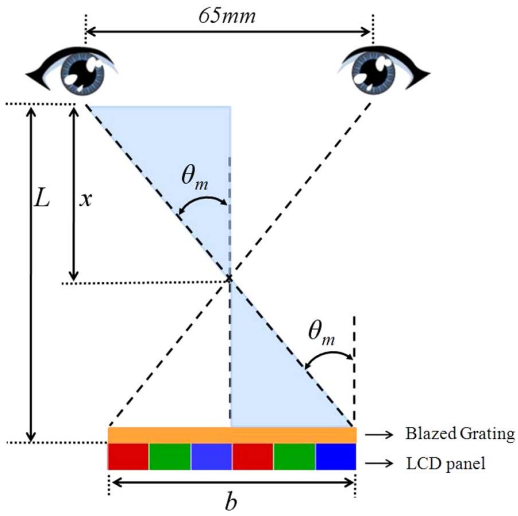

Fig. 1. Relationship between the viewing distance and the panel.

II. Design

The diffractive splitter is a symmetric blazed grating [3] that aims to deliver the image at the left FOV on an LCD panel to the left eye of a human being and image at the right FOV to the right eye; it also aims to generate depth perception using the disparity between the left and right FOV. As blazed gratings are sensitive

Manuscript received June 04, 2011; revised September 27, 2011, March 08, 2012, April 02, 2012; accepted April 06, 2012. Date of publication June 21, 2012; date of current version June 28, 2012. This work was supported by the National Science Council of Taiwan under Contract NSC 98-2221-E-224-007.

C.-Y. Chen is with the Department of Electronics Engineering, National Yunlin University of Science and Technology, Douliou, Yunlin 64002, Taiwan (e-mail: chencyue@yuntech.edu.tw).

Q.-L. Deng is with the Institute of Photonic Systems, National Chiao Tung University, Tainan County 71150, Taiwan (e-mail: parite.deng@gmail.com).

B.-S. Lin is with the Institute of Imaging and Biomedical Photonics, National Chiao Tung University, Tainan County 71150, Taiwan (e-mail: borshyhlin@gmail.com).

W.-C. Hung was with the Graduate School of Optoelectronics, National Yunlin University of Science and Technology, Douliou, Yunlin 64002, Taiwan (e-mail: g9618720@yuntech.edu.tw).

Color versions of one or more of the figures are available online at http://ieeexplore.ieee.org.

Digital Object Identifier 10.1109/JDT.2012.2194984

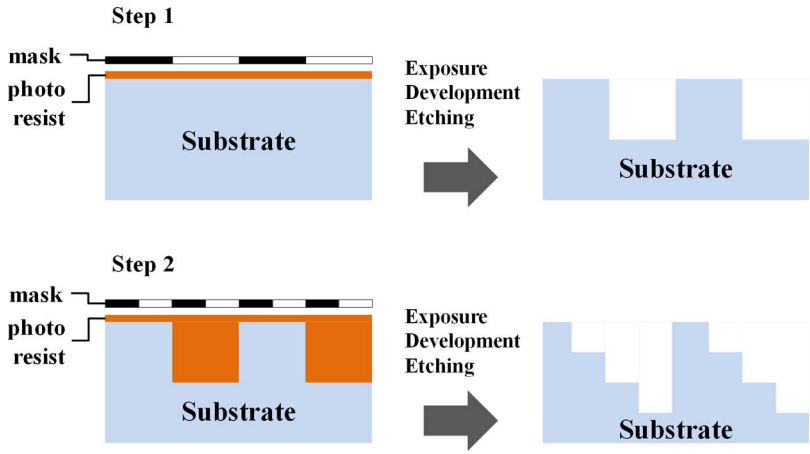

Fig. 2. Production of four-stage phase grating.

TABLE I
PARAMETERS FOR THE REFERENCE PANEL

Panel size (inches)	Resolution (pixels)	Sub-pixel size (μm)	Wavelength(nm)		
			Red	Green	Blue
2.2	176x220	66	596	554	450

TABLE II
DIFFRACTION EFFICIENCY OF THE MULTISTAGE FABRICATION

	4-level phase	8-level phase	16-level phase
First order	79.0%	89.3%	90.1%
Other order	5.3%	1.0%	0.6%
Differences	73.7%	88.3%	89.5%

to wavelength, the pitch of the gratings is related to the sub-pixels of the panels to reduce the crosstalk commonly found in stereoscopic display technology. The parameters for the applied panel are shown in Table I. From Fig. 1, the diffractive angle θ_m of the diffractive elements is represented by the cross disparity exhibited when viewing the stereoscopic images. As a result, when the viewing distance L cm, reference panel width b cm, and relative coefficient x cm are determined, the blazed grating pitches and blazing angles corresponding with red, green, and blue light can be calculated based on the following equations:

$$T = \frac{m\lambda}{\sin\left\{\tan^{-1}\left[\frac{b}{2(L-x)}\right]\right\}} \tag{1}$$

$$\theta_b = \tan^{-1}\left(\frac{n_s - \cos\theta_m}{\sin\theta_m}\right) \tag{2}$$

where m is the diffractive order, λ is the wavelength, T is the pitch of the blazed grating, θ_b is the base angle of the blazed grating, and n_s is the refractive index of the blazed grating.

III. FABRICATION

The semiconductor technology currently used to produce diffractive optical elements is well developed. The blazed grating process was applied using photolithography and reactive ion etching (RIE) to produce the four-stage phase blazed grating used in this study [7]. The diffraction efficiencies achieved during the four stages of the process are shown in Table II. When the binary optical element is at the fourth stage, the first-order diffraction efficiency was 79.0%, and at the second-stage, the efficiency was 5.3%, approximately 15 times less. At stage sixteen, the first-order diffraction efficiency achieved was 90.1%. However, with RIE, the elements have more stages; therefore, the process is more difficult, and more errors result. The requirement for precision then becomes stricter. Considering the feasibility of the technology, the blazed grating was produced in four stages. The 79.0% first-order diffraction efficiency has a fourfold higher brightness than the barrier type used in traditional displays [1]. Using the above binary staging, two masks were required for the surface of the four-stage elements. The procedure is shown in Fig. 2.

A. Initial Mask Design

The 5″ chrome-plated quartz mask (127 mm×127 mm) used was produced by the Taiwan Mask Corporation. Using (1) and (2), the blazed grating pitches calculated for red, green, and blue light were 9.00, 8.40, and 6.80 μm, respectively. Binary staging was applied to produce four-stage masks in which the trace width of the first mask was half of the grating pitch. Therefore, the pitches for red, green, and blue (RGB) in the first mask were 4.50, 4.20, and 3.40 μm, respectively (Fig. 3). Similarly, the trace width of the second mask was half that of the first mask, in which the pitches of RGB were 2.25, 2.10, and 1.70 μm, respectively (Fig. 4). During the blazed grating process, the quality depends on the alignment accuracy of the two masks. When the masks are not aligned, the blazed grating structure is damaged completely, and this further affects the diffractive splitting. In this case, the corresponding alignment keys of the two masks are separately drawn at 30 μm×30 μm. Moreover, to reduce errors in rollover and injection, quartz, which can directly transmit light, was selected as the material for the DOE. Using RIE, the splitting efficiency of the stereoscopic image pairs could be directly measured and obtained. The most efficient process was achieved by: 1) reducing the number of process steps; 2) reducing the time; and 3) reducing the cost. Nonetheless, alignment of the two masks on transparent substrates is considerably difficult to achieve. This study therefore proposed alignment of the masks on transparent substrates to effectively enhance the process yield.

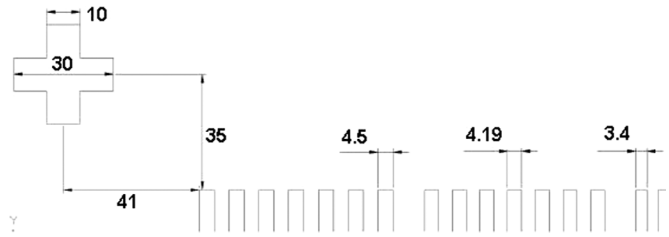

Fig. 3. Detailed design of the initial mask (mask-1).

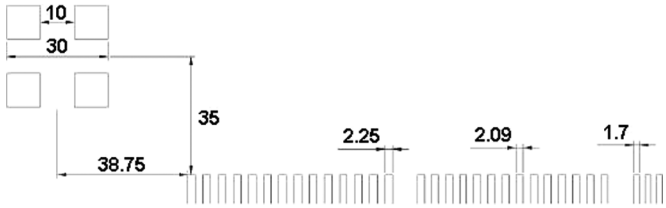

Fig. 4. Detailed design of the initial mask (mask-2).

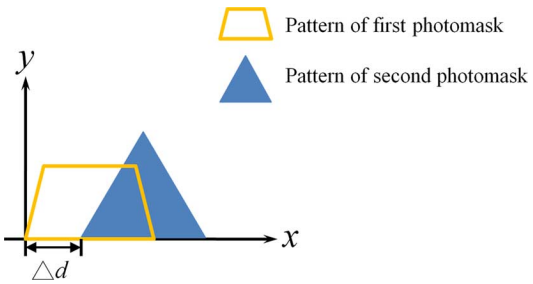

Fig. 5. Relative shift between the masks.

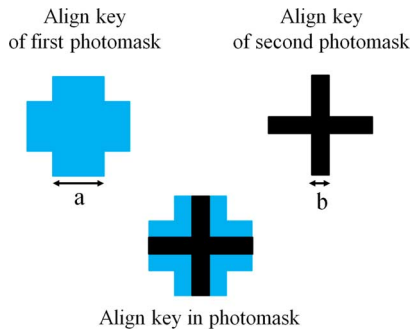

Fig. 6. Alignment key in the mask.

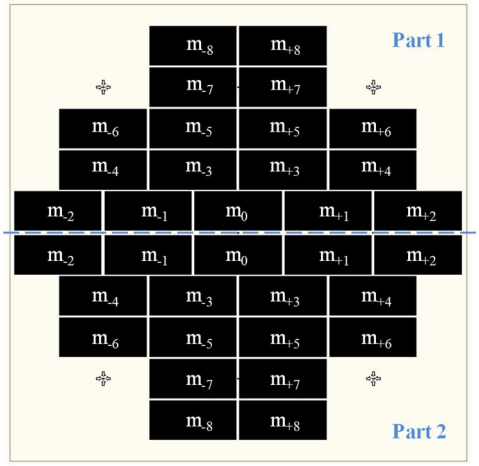

Fig. 7. Modified mask design (mask-2).

B. Modified Mask Design

Because it was difficult to align the two quartz photo-masks and because machine error can affect the diffraction of the components, low-frequency vibration resulting from the equipment was likely to change the position of the two photo-masks even when aligned. Consequently, the experiment was modified. Indirectly using the tolerance between the alignment keys of the two photo-masks as the parameter, the maximal relative displacement of Δd within the two photo-masks was defined (Fig. 5).

However, m_n sets of patterns, $m_0, m_{+1}, m_{-1}, \ldots, m_{(+n)}, m_{(-n)}$, were designed for the photo-mask to enhance one or more effective patterns in the experiments (n was the displacement of the second photo-mask, which was defined as positive when moving horizontally toward $+x$ and vice versa). The maximal relative displacement Δdm_n was calculated using

$$\Delta dm_n = 2 \times n \times \mathrm{Me} \times t \tag{3}$$

where the maximum error (Me) is the percentage of the maximal tolerance of alignment and t is the minimum structural period of the blazed grating.

Depending on the size of the alignment key, the number of the effective patterns on the photo-mask could further affect the change of the relative displacement. In this case, when Δdm_n satisfied (4) and the alignment keys of the first and second photo-masks were aligned (see Fig. 6), one of the effective patterns would completely correspond

$$|\Delta dm_n| \leq \frac{(a-b)}{2} \tag{4}$$

where a is the size of the alignment key of the first photo-mask and b is the size of the alignment key of the second photo-mask.

Having satisfied (3) and (4), 17 patterns, which included 8 positive shifting patterns, 8 negative shifting patterns, and 1 original pattern, were designed on the mask (Fig. 7). Moreover, two sets of symmetrical patterns were designed on the mask to increase the number of effective patterns in the process (the horizontal dashed line in Fig. 7 was the axis of symmetry), showing that two effective patterns would be acquired.

C. Process Procedure

Having confirmed the alignment of the quartz masks, a 4″ quartz plate with a visible optical wave (0.38–0.78 μm) and transmission greater than 91% was selected. RIE was further applied to produce a blazed grating. The positive photo resist AZ 5214 was first coated well onto the quartz plate. The first mask exposure was exposed to UV light (365 nm). KTD-1 was further utilized for development and fixation. Finally, the surface pattern was etched using ion etching. Having confirmed the pattern of the first mask and repeated the above steps, the pattern etching of the second mask was completed. With the effective alignment design, the experimental time and cost of the process were remarkably reduced.

TABLE III
BLAZED GRATING ELEMENT PARAMETERS OF RGB

Sub-pixel	Refractive index	Period(μm)	Depth(μm)	Blazed angle(°)
Red	n_R=1.458	9.00	1.02	6.50
Green	n_G=1.460	8.40	1.02	6.90
Blue	n_B=1.480	6.80	1.02	8.50

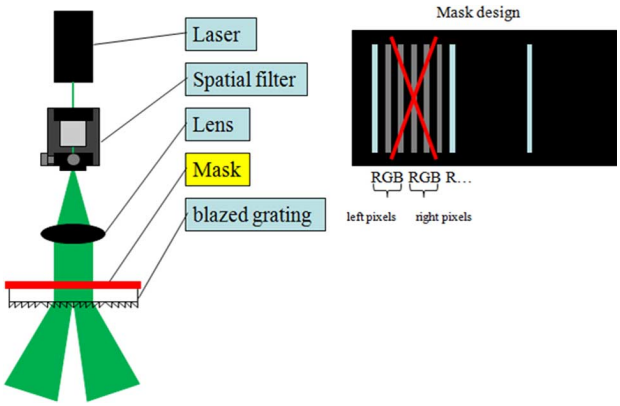

Fig. 8. Efficiency measurement.

Using reactive ion etching, the depths of the etched patterns were identical. Based on the mask's minimal trace width of 1.70 μm, the maximally average diffraction efficiency of RGB for the blazed grating was utilized to select the optimal process depth. When calculated using *Gsolver* for a process depth of 1.02 μm, a maximally average diffraction efficiency of 74.3% was achieved. The blazed grating structure RGB parameters under these conditions are shown in Table III.

IV. RESULTS

Having completed the blazed grating, the diffraction efficiency and splitting angle were measured for comparison with the requirements of autostereoscopic displays. Based on the efficiency measuring system presented in Fig. 8 and to accurately measure the relative diffraction efficiency, the individual diffraction efficiency measurement was added to the masks to cover the sub-pixels, as the micro-structure of the RGB gratings is designed using the same diffractive elements. First, using a laser set to the wavelength of 633 nm, which passed through a parallel beam expanding system and illuminated the red component of the left sub-pixel with the measuring mask, the $+1$ grating diffraction efficiency was measured. Moving the mask to the green component of the next left sub-pixel, the $+1$ grating diffraction efficiency was measured again using a 532-nm laser. Then, the $+1$ grating diffraction efficiency of the blue component of the next left sub-pixel was measured using a 432-nm laser. Similarly, the $+1$ grating diffraction efficiency of RGB of the right sub-pixel was measured by repeating the above steps. Tables IV–VI present the diffraction efficiency of the RGB structures of the left and right FOV.

An experimental setup was shown as Fig. 9 was used to demonstrate a stereogram implemented with the proposed quartz blazed grating. The blazed grating was attached on a 2.2-in LCD and it was carefully aligned with the display pixels. We found the spatial-multiplexed image prepared for stereo-effect on LCD was effectively separated via the quartz blazed grating and this leaded to a stereoscopic vision with an around 25 cm viewing distance for observers. The separated right and left images were individually captured by CCD cameras, and they were also shown in Fig. 9.

TABLE IV
DIFFRACTION EFFICIENCY OF RED

Incident light intensity 51.23μW	+1	0	-1
Fabricated diffraction efficiency	69.70%	9.30%	1.70%
Real value of the left FOV	19.81μW	6.91μW	8.35μW
Diffraction efficiency of the left FOV	38.70%	13.50%	16.30%
Real value of the right FOV	22.98μW	9.63μW	7.47μW
Diffraction efficiency of the right FOV	44.90%	18.80%	14.60%

TABLE V
DIFFRACTION EFFICIENCY OF GLEEN

Incident light intensity 9.31μW	+1	0	-1
Fabricated diffraction efficiency	78.60%	1.90%	0.50%
Real value of the left FOV	4.64μW	0.48μW	0.70μW
Diffraction efficiency of the left FOV	49.80%	5.20%	7.60%
Real value of the right FOV	5.15μW	0.44μW	0.86μW
Diffraction efficiency of the right FOV	55.30%	4.80%	9.30%

TABLE VI
DIFFRACTION EFFICIENCY OF BLUE

Incident light intensity 5.65μW	+1	0	-1
Fabricated diffraction efficiency	69.70%	0.30%	0.10%
Real value of the left FOV	2.34μW	0.07μW	0.30μW
Diffraction efficiency of the left FOV	41.40%	1.30%	5.40%
Real value of the right FOV	1.91μW	0.08μW	0.15μW
Diffraction efficiency of the right FOV	33.80%	1.50%	2.70%

V. DISCUSSION

This study utilized reactive ion etching on transparent quartz substrates to produce DOEs for autostereoscopic displays. To replace traditional micromachining technology, the process needed to overcome the cumulative errors caused by using multiple steps, as with LIGA. The blazed grating was produced using quartz substrates such that the images could be formed after two ion etchings and attached to displays to demonstrate the effect of the autostereoscopic displays. However, the transparent substrate could be subject to a serious alignment problem. In general, when aligning the second mask on a quartz plate, the first etching is likely to damage the alignment key, thereby causing ineffective alignment. For this reason, we proposed a solution to the problem of multistage alignment on transparent substrates to enhance the alignment key size for easier alignment. This solution would also increase the tolerance of the alignment, thereby reducing the loss in the process.

Based on previous research, the metal alignment key on the quartz plate was first coated; however, an additional mask was required to define the alignment key position. A 2^n-stage phase grating requires $2n$ masks and $(2n-1)$ alignments, and these complex steps would greatly reduce the production efficiency

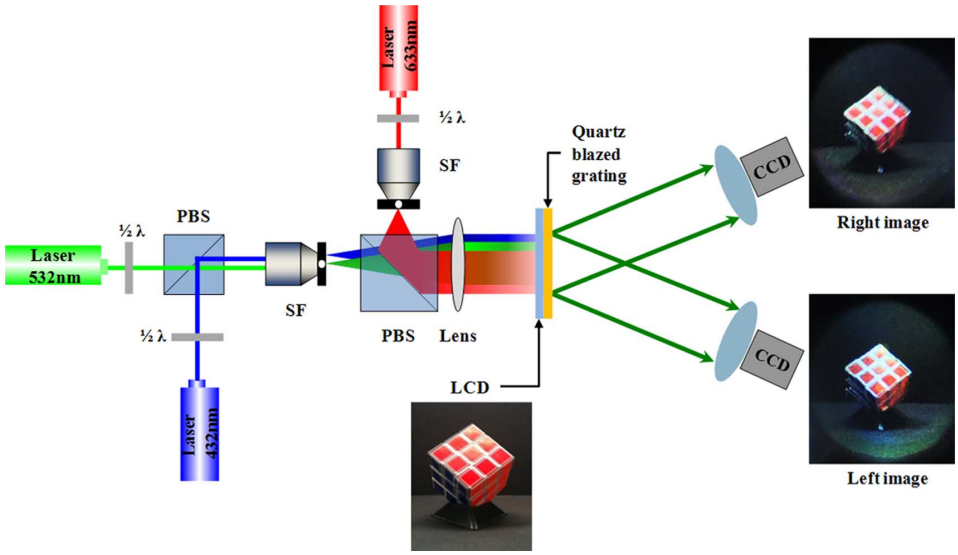

Fig. 9. Experimental architecture for implementing a stereogram using the proposed quartz blazed grating.

and cause further errors. By using only n masks and $(n-1)$ alignments, the blazed grating can be effectively produced without the hot sputtering process.

Furthermore, based on (3) and (4), the blazed grating pattern in the mask produced 17 symmetric pairs (see Fig. 7). The maximal tolerance of Me was 9%, the minimal structure pitch was 6.80 μm, and the alignment key widths of the two masks were 30 μm and 10 μm. The maximal relative displacement was 9.79 μm. Using a correctly aligned symmetric arrangement, two sets of blazed gratings were successfully produced, thereby reducing costs and enhancing process efficiency.

Having completed the production, the measuring structure illustrated in Fig. 8 was applied to analyze the diffraction efficiency and evaluate the brightness requirement of the autostereoscopic displays. As shown in Tables IV–VI, when measuring red light (633 nm), the $+1$ grating average diffraction efficiency of the left and right FOV was 41.80%; when measuring green light (532 nm), the $+1$ grating average diffraction efficiency of the left and right FOV was 52.55%; and when measuring blue light (442 nm), the $+1$ grating average diffraction efficiency of the left and right FOV was 37.60%. Green light exhibited the highest diffraction efficiency, and blue light showed the least. Brightness was enhanced up to 1.68–2.47-fold higher compared with barrier type autostereoscopic displays [1].

In stereoscopic display technology, the left image is delivered to the left eye, and the right image is sent to the right eye. When one eye receives too much information assigned to the other eye, interference results. The eyes would therefore see the same image, resulting in point crosstalk. To verify the crosstalk of the produced blazed grating, which was attached behind the panel, we utilized the contrast ratio (CR) parameter to define the effect of crosstalk using (5). Based on the literature, when CR is less than the critical value of 0.1, interference is large. However, interference is less when CR is greater than this critical value [8]–[10]. First, the CR of the left FOV was calculated. The photometer was fixed on the $+1$ grating light angle of the left FOV to measure the $+1$ grating diffraction light intensity $(L_{\max})$. Moving the measuring mask such that the incident light merely illuminated the right FOV, the diffraction light intensity of the left FOV $(L_{\min})$ was measured. The results, based on (5), are shown in Table VII. Similarly, the CR of the right FOV was obtained using similar steps, as shown in Table VIII.

TABLE VII
CR OF THE LEFT FOV

Wavelength	L_{max}	L_{min}	CR
633nm	19.81	2.76	0.76
532nm	4.64	0.11	0.95
442nm	2.34	0.52	0.64

TABLE VIII
CR OF THE RIGHT FOV

Wavelength	L_{max}	L_{min}	CR
633nm	22.98	2.49	0.80
532nm	5.15	0.12	0.95
442nm	1.91	0.21	0.80

$$\mathrm{CR} = \frac{(L_{\max} - L_{\min})}{(L_{\max} + L_{\min})}. \tag{5}$$

From Tables VII and VIII, the maximal and minimal CRs of the left FOV were 0.95 and 0.64, respectively, and the maximal and minimal CRs of the right FOV were 0.95 and 0.80, respectively. The outcomes of the left and right FOV were both larger than the critical value of 0.1; therefore, the produced blazed grating crosstalk did interfere in the left and right FOV when used for splitting. The produced blazed grating could therefore act as an excellent splitter for stereoscopic displays.

VI. CONCLUSION

To implement the application of blazed grating in diffractive elements to the splitter of autostereoscopic displays, this study applied photolithography and RIE to produce a blazed grating that avoided the cumulative errors that result from the general

LIGA process. Selecting quartz as the substrate, a four-stage structure was designed to consider the feasibility of this process. A method for alignment on transparent substrates was also proposed to greatly enhance the process efficiency. Having completed the four-stage blazed grating, an optimal diffraction efficiency of 55.30% was measured for green light, and the overall efficiency ranged from 1.68-fold to 2.47-fold higher than that of traditional barrier type autostereoscopic displays. Furthermore, based on an evaluation of crosstalk, the CR values of the left and right FOV of the delivered stereoscopic images were larger than the defined critical value. This performance indicates that the blazed grating used in a DOE could be applied to plane displays to achieve the splitting effect required in autostereoscopic displays.

REFERENCES

[1] C. Y. Chen, M. C. Chang, M. D. Ke, C. C. Lin, and Y. M. Chen, "A novel high brightness parallax barrier stereoscopy technology using a reflective crown grating," *Microw. Opt. Technol. Lett.*, vol. 50, pp. 1610–1616, Jun. 2008.

[2] C. Y. Chen, T. Y. Hsieh, J. R. Sze, and W. C. Su, "Design and fabrication of quartz-based micro prism array of dual-view display by using reactive ion etching," in *Proc. SPIE*, 2008, vol. 7001, p. 70010N.

[3] C. Y. Chen, Q. L. Deng, and H. C. Wu, "A high-brightness diffractive stereoscopic display technology," *Displays*, vol. 31, pp. 169–174, 2010.

[4] H. Morishima, H. Nose, N. Taniguchi, K. Inoguchi, and S. Matsumura, "Rear-cross-lenticular 3D display without eyeglasses," in *Proc. SPIE*, 1998, vol. 3295, no. 193.

[5] M. G. Moharam and T. K. Gaylord, "Rigorous coupled-wave analysis of planar-grating diffraction," *J. Opt. Soc. Amer.*, vol. 71, no. 7, pp. 811–818, July 1981.

[6] E. W. Becker, W. Ehrfeld, P. Hagmann, A. Maner, and D. Munchmeyer, "Fabrication of microstructures with high aspect ratios and great structural heights by synchrotron radiation lithography, galvanoforming, and plastic molding (LIGA process)," *Microelectron. Eng.*, vol. 4, pp. 35–56, 1986.

[7] G. J. Swanson and W. B. Veldkamp, "Diffractive optical elements for use in infrared systems," *Opt. Eng.*, vol. 28, pp. 605–608, 1989.

[8] K. Teunissen, S. Qin, and I. Heynderickx, "A perceptually based metric to characterize the viewing-angle range of matrix displays," *J. Soc. Inf. Display*, vol. 16, no. 1, pp. 27–36, 2008.

[9] C. Y. Chen, T. Y. Hsieh, Q. L. Deng, W. C. Su, and Z. S. Cheng, "Design of a novel symmetric microprism array for dual-view display," *Displays*, vol. 31, pp. 99–103, 2010.

[10] W. C. Su, C. Y. Chen, and Y. F. Wang, "Stereogram implemented with a holographic image splitter," *Opt. Express*, vol. 19, no. 10, pp. 9942–9949, 2011.

Chien-Yue Chen was born in Taitung, Taiwan, 1969. He received the B.S. degree in physics from Soochow University, Taipei, Taiwan, in 1992, and the M.S. and Ph.D. degrees in space science and optical science individually, from National Central University, Nanking, China, in 1994 and 2004, respectively.

He is currently an Associate Professor at the Department of Electronics Engineering, National Yunlin University of Science and Technology, Yunlin, Taiwan. His research interests include optical design, micro-optics and 3D displays.

Qing-Long Deng received the B.S. and M.S degrees in electronic engineering and optoelectronic engineering individually, from National Yunlin University of Science and Technology, Yunlin, Taiwan, in 2008 and 2010, respectively, and is currently working toward the Ph.D. degree from Institute of Photonic Systems, National Chiao Tung University.

His research interests include autostereoscopic, optical design and optical information processing.

Bor-Shyh Lin received the B.S. degree from NCTU, Taiwan, in 1997, M.S. degree in electrical engineering from National Taiwan University (NTU), Taiwan, in 1999, and Ph.D. degree in electrical engineering from NTU, Taiwan, in 2006.

He is currently Assistant Professor of the Institute of Imaging and Biomedical Photonics, National Chiao Tung University (NCTU), Taiwan. His research interests are in the areas of biomedical circuits and systems, biomedical signal processing, and biosensor.

Wen-Cheng Hung received the B.S. degree in optical science Minghsin University of Science and Technology in 2007, and the M.S. degree in optoelectronic engineering from National Yunlin University of Science and Technology, Yunlin, Taiwan, in 2010.

His research interests include lens design, optical design, and autostereoscopic.